


Article

Co-Gasification Characteristics of Coal and Biomass Using CO₂ Reactant under Thermodynamic Equilibrium Modelling

M. Shahabuddin ^{1,2,*}  and Sankar Bhattacharya ¹ 

¹ Department of Chemical Engineering, Monash University, Wellington Rd, Clayton 3800, Australia; sankar.bhattacharya@monash.edu

² Department of Mechanical Engineering and Product Design Engineering, Swinburne University of Technology, Hawthorn 3122, Australia

* Correspondence: s.ahmmad@federation.edu.au or sahammad@swinburne.edu.au

Abstract: This study assessed the entrained flow co-gasification characteristics of coal and biomass using thermodynamic equilibrium modelling. The model was validated against entrained flow gasifier data published in the literature. The gasification performance was evaluated under different operating conditions, such as equivalence ratio, temperature, pressure and coal to biomass ratio. It is observed that the lower heating value (LHV) and cold gas efficiency (CGE) increase with increasing temperature until the process reaches a steady state. The effect of pressure on syngas composition is dominant only at non-steady state conditions (<1100 °C). The variation in syngas composition is minor up to the blending of 50% biomass (PB50). However, the PB50 shows a higher LHV and CGE than pure coal by 12% and 18%, respectively. Overall, biomass blending of up to 50% favours gasification performance with an LHV of 12 MJ/kg and a CGE of 78%.

Keywords: co-gasification; CO₂ reactant; coal; biomass; syngas; aspen plus modelling



Citation: Shahabuddin, M.; Bhattacharya, S. Co-Gasification Characteristics of Coal and Biomass Using CO₂ Reactant under Thermodynamic Equilibrium Modelling. *Energies* **2021**, *14*, 7384. <https://doi.org/10.3390/en14217384>

Academic Editors: Fernando Rubiera González and Michael Pohorelý

Received: 11 September 2021
Accepted: 1 November 2021
Published: 5 November 2021

Publisher's Note: MDPI stays neutral with regard to jurisdictional claims in published maps and institutional affiliations.



Copyright: © 2021 by the authors. Licensee MDPI, Basel, Switzerland. This article is an open access article distributed under the terms and conditions of the Creative Commons Attribution (CC BY) license (<https://creativecommons.org/licenses/by/4.0/>).

1. Introduction

Since the industrial revolution in 1750, CO₂ in the atmosphere has increased by 45%, resulting in climate change and global warming [1]. The main contributor to CO₂ emission is power generation, accounting for 39.7%, followed by industry, transport, building and others with 25%, 21.2%, 8.5% and 5.6%, respectively [2]. As the second-largest source of power generation, coal emits 41% of total CO₂ worldwide [2]. Hence, various technologies have been employed to reduce, capture and utilise CO₂ from power generation. One such technique is integrated gasification combined cycle (IGCC) power generation with carbon capture and storage (CCS) [3].

The gasification produces syngas (CO, H₂, CH₄ and CO₂, etc.) by partial oxidation of carbonaceous solid fuels such as coal and biomass [4]. The syngas generated from gasification is used for power generation using gas turbines and chemical synthesis with appropriate downstream treatment [5]. CO₂ generated from gasification plants can be reused in the same cycle as a reactant, which helps cut costly oxygen-enriched air, oxygen and steam [6]. Thus, besides environmental benefits, the cost of producing steam and oxygen from air separation units can be reduced substantially [7]. Furthermore, the recycling of CO₂ offers a wide range of CO/H₂ production, which is the precursor for a wide range of chemicals [8].

Numerous studies on coal and biomass gasification have been conducted using CO₂ as a reactant [9–15]. The objectives of those investigations were kinetic studies [13,16], gas composition and subsequent char/ash characterisation [10,17] and fluid dynamic and process modelling [18–20]. The kinetic parameters are useful for understanding the reactivity of the fuels, which helps set the operating conditions for pilot scale analysis. Besides, the kinetic parameters are also important for fluid dynamics and process modelling studies [13]. The pilot-scale studies are crucial to assess the performance characteristics

of the gasifier and operating conditions [21]. The process modelling is particularly vital, capable of providing a wide range of data while eliminating the need for time and costly experimental campaigns [22].

Shahabuddin et al. [22] studied the gasification characteristics of bituminous coal using a process modelling approach under different reactants, such as oxygen, steam, CO₂ and a mixture of those. Results showed that the combination of steam and oxygen performs better compared to other reactants. The steam–oxygen reactant showed the highest H₂/CO ratio of 0.74, while the ratio was about 0.32 using steam–CO₂ and pure oxygen. Sadhwani et al. [18] studied Aspen plus process modelling for the gasification of biomass using CO₂ reactant with known kinetics. The results were validated with experimental data and found a co-efficient of determination between 84.38% and 98.72% for gas compositions under different operating conditions. The co-gasification of coal and biomass is gaining popularity due to its favourable impact on carbon conversion, gas quality and emission, thus making the system more environmentally benign [23,24]. Ali et al. [25] studied entrained flow co-gasification of different coals and rice straw biomass using Aspen plus process modelling. Among the different blending ratios tested, a 10% addition of biomass showed the best gasification performance with a CGE of 78.5%.

Similarly, Kuo and Wu [26] studied the co-gasification characteristics of coal and biomass using Aspen plus thermodynamic equilibrium modelling under steam gasification conditions along with a certain percentage of CO₂. Results showed that the addition of CO₂ improves energy conversion and exergy efficiency. A reduction in CO₂ emission by 38% was reported by co-gasification compared to pure coal gasification.

Despite some thermodynamic modelling for the co-gasification of coal and biomass using CO₂ reactants partially, limited or no studies are available on the co-gasification characteristics of coal and biomass using pure CO₂ reactants (ex situ) under thermodynamic equilibrium modelling, especially under entrained flow conditions [8,27]. Besides developing fuel-specific data, this process modelling has studied the effect of coal (Barapukurian bituminous coal) and pine bark (*Pinus Radiata*) biomass ratio on the gasification performance. In addition, various performance parameters such as carbon conversion, H₂/CO ratio, heating value and cold gas efficiency have been analysed under different operating conditions.

2. Methodology

This study investigated the steady state co-gasification behaviour of coal and biomass under CO₂ gasification conditions using Aspen plus process simulator. The following sections describe the theoretical background, simulation approach, assumptions and validation of the thermodynamic equilibrium model.

2.1. Theoretical Background

The current process modelling consists of the decomposition of fuel, gasification and equilibrium calculation, as shown in the process flow sheet (Figure 1). The decomposition of coal and biomass takes place in the RYield reactor. The RYield reactor works with the principle of known yield composition, where reaction stoichiometry is not known [28]. The yield composition is given according to the proximate and ultimate data of the fuel samples. In addition, the enthalpy liberated due to the decomposition was based on the heating value of the sample. After decomposition, the elements are oxidised partially with a sub-stoichiometric oxygen supply. Various homogenous and heterogeneous reactions, reported in Table 1, occur in the RGibbs reactor [22,29].

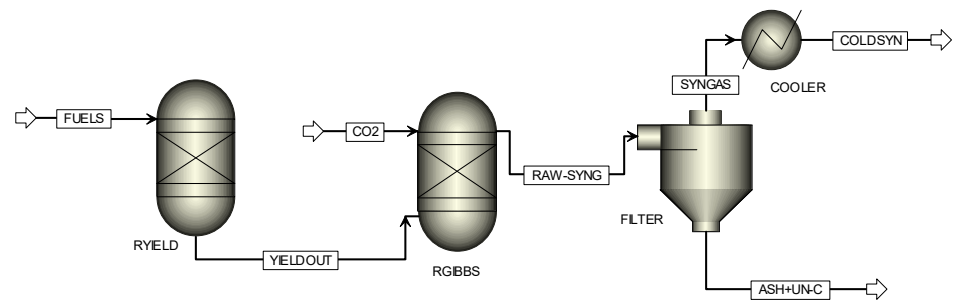


Figure 1. Process flow sheet of the thermodynamic equilibrium model.

Table 1. Major gasification reactions (adapted with permission from [22]).

Reaction Name	Chemical Formula	Enthalpy ($\frac{\text{KJ}}{\text{mol}}$)	Eq. No.
Boudouard reaction	$\text{C}_{(s)} + \text{CO}_2 \rightarrow 2\text{CO}$	$(\Delta H = +159.7)$	(1)
Steam gasification	$\text{C}_{(s)} + \text{H}_2\text{O} \rightleftharpoons \text{CO} + \text{H}_2$	$(\Delta H = +118.9)$	(2)
Hydrogen combustion	$\text{C}_{(s)} + 2\text{H}_2 \rightleftharpoons \text{CH}_4$	$(\Delta H = -88.4)$	(3)
Water-gas shift reaction	$\text{CO} + \text{H}_2\text{O} \rightleftharpoons \text{CO}_2 + \text{H}_2$	$(\Delta H = -41.1)$	(4)
Steam methane reforming	$\text{CH}_4 + \text{H}_2\text{O} \rightleftharpoons \text{CO} + 3\text{H}_2$	$(\Delta H = +206.3)$	(5)
Dry methane reforming	$\text{CH}_4 + \text{CO}_2 \rightleftharpoons 2\text{CO} + 2\text{H}_2$	$(\Delta H = -247)$	(6)
Sabatier reaction	$\text{CO}_2 + 4\text{H}_2 \rightleftharpoons \text{CH}_4 + 2\text{H}_2\text{O}$	$(\Delta H = +73)$	(7)

The RGibbs reactor does not need any chemical reaction to be defined. However, it requires operating temperature and pressure to determine possible product compositions under chemical and phase equilibrium. Due to the sub-stoichiometric oxygen supply, carbon may not burn fully. The unburnt carbon and ash are filtered out using a filter in the subsequent stage [30]. After that, the syngas from another filter stream is cooled down using a cooler to a temperature typically used for steam reforming. The details of the unit blocks used in the process modelling are explained in Table 2.

Table 2. Description of the unit blocks used in the process modelling [28].

Type	Model	Schematic	Descriptions and Operating Conditions
Reactors	RYield		This unit is used as a decomposition reactor to break down coal/biomass into components based on the proximate and ultimate data. This reactor is used when component yield distribution is the only known parameter. This reactor is isothermal, and the operating parameters for this reactor are temperature and pressure.
	RGibbs		This equilibrium reactor works based on rigorous or multiphase equilibrium according to the Gibbs free energy minimisation technique, subject to atom balance constraints. This model does not require reaction stoichiometry or reaction kinetics to be specified and can determine phase equilibrium without any chemical reaction. The operating parameters are either temperature and pressure or pressure and enthalpy. This model is used for thermodynamic equilibrium calculation in the gasifier to determine the final syngas composition.
Filter	SSplit		The SSplit is the sub-stream splitter. This unit divides feed based on splits specified for each sub-stream. The operating parameter for this unit is split fraction. The current modelling study used this unit to separate ash and unburnt carbon from the syngas.
Heat Exchangers	Cooler		This unit is the thermal and phase state changer, which can model heater, cooler and condenser. The operating parameters for this unit are temperature and pressure. In this study, this unit is used to drop the hot syngas temperature to 225 °C—a typical temperature used in steam reforming to produce hydrogen.

2.2. Model Description and Simulation Procedures

This thermodynamic equilibrium study uses commercial Aspen plus process modelling software, with version V10. The details of the simulation procedures are described in our earlier publication [22]. Hence, only a synopsis of the modelling procedures is described here. The simulation performs mass and energy balance to reach chemical equilibrium. This software features an inbuilt physical, chemical and thermodynamic database for different elements [31]. In this study, the Peng–Robinson–Boston–Mathias (PR–BM) property method is used due to its ability to model non-ideal behaviour under high-temperature entrained flow conditions [25,32]. In Aspen plus simulation, coal and ash were defined as nonconventional components (NC), while conventional components include elemental compositions, CO, H₂, CH₄, CO₂, H₂O, H₂S and HN₃. The NC components were defined based on the proximate and ultimate data of the fuels, as shown in Table 3. HCOALGEN and DCOALIGT features of the software were used to model the enthalpy and density of the nonconventional components.

Table 3. Chemical properties of coal and biomass samples (wt.%, dry basis).

Sample *	Proximate Analysis				Ultimate Analysis					LHV (MJ/kg)	
	Moisture	VM	FC	Ash	C	H	N	S	O		Ash
PB0	3.10	30.61	57.79	11.60	74.19	4.59	1.52	0.55	7.55	11.60	30.26
PB20	3.13	37.69	52.81	9.50	67.57	5.12	1.15	0.38	16.28	9.50	27.72
PB50	3.17	48.31	45.39	6.30	62.51	5.63	0.78	0.23	24.55	6.30	23.91
PB80	3.20	58.92	37.88	3.20	57.29	6.21	0.36	0.08	32.86	3.20	20.09
PB100	3.23	66.02	32.88	1.10	53.89	6.54	0.14	0.01	38.32	1.10	17.55

* The numerical value in the sample name denotes its percentage of pine bark biomass (PB), which is balanced to 100% with coal.

2.3. Assumption of the Model

The following assumptions are made to model complex entrained flow gasification:

- The gasifier is steady state and isothermal [25]
- The residence time is sufficiently long to reach chemical equilibrium [33]
- A gasifier heat loss of 2.0% is considered with no pressure loss from the system [34,35]
- The major pyrolysis product consists of H₂, CO, CH₄, CO₂ and H₂O, which are instantaneous [25,36]
- Gasification does not produce any NO_x or tar under a high-temperature CO₂ atmosphere [37]
- There is no separate purge or fuel-conveying gas in the system. CO₂ is used as a purge or fuel-conveying gas, which is accounted for in the CO₂ stream of the process flow sheet
- Ash does not take part in chemical reactions [25,36]

2.4. Model Validation

The validation of the model was firstly carried out against Texaco entrained flow gasifier data under various operating conditions. The operating conditions reported in Table 4 are adapted from Ref. [25], originally collected from Ref. [31]. The current model was further verified against our large bench-scale entrained flow gasifier data at 1000 °C, as published in the literature [22]. The key operating conditions were 1 gm/min of fuel flow, 12.0 L/min of CO₂ and 4.0 L/min of purge N₂. However, the details of the reactor configurations and other operating conditions can be found in Ref. [38].

Table 4. Operating conditions of Texaco entrained flow gasifier (adapted with permission from [25]).

Run	Feed Rate (kg/h)			Reactant/Fuel Ratio	
	Fuel	O ₂	Steam	O ₂ /Fuel	Steam/Fuel
Run-1	275.976	238.995	66.510	0.866	0.241
Run-2	292.248	224.446	92.935	0.768	0.318
Run-3	295.920	240.583	91.439	0.813	0.309
Run-4	286.056	230.847	92.396	0.807	0.323
Run-5	257.804	212.946	90.747	0.826	0.352
Run-6	315.828	244.451	91.906	0.774	0.291
Run-7	327.492	254.134	92.353	0.776	0.282
Run-8	331.668	264.339	81.922	0.797	0.247
Run-9	316.044	248.727	84.700	0.787	0.268

The syngas composition (dry basis), presented in Figure 2, shows that the results obtained from the current model agree with those from the literature. Some discrepancies between the experimental and modelling results are due to the simplification in modelling and error in experimental measurements. Following model validation, a range of sensitivity studies has been carried out under various operating conditions.

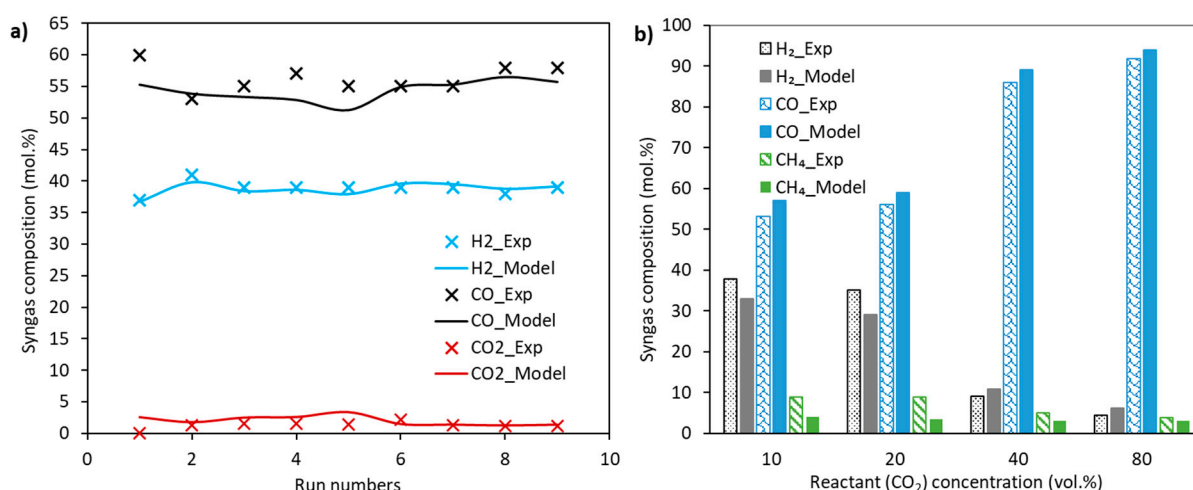


Figure 2. Model validation against (a) commercial-scale Texaco gasifier (adapted with permission from [25]) and (b) large bench-scale entrained flow gasifier data (adapted with permission from [22]).

3. Results and Discussions

3.1. Effect of Equivalence Ratio on the Gasification Performance of Coal

Figure 3 shows the effect of equivalence ratio (ER, ϕ) on carbon conversion at various gasifier temperatures (T_g). It can be seen that increasing the equivalence ratio increases the carbon conversion [39]. The result also indicates that the carbon conversion increases with increasing temperatures [7]. Apparently, at a temperature of 1100 °C, available CO₂ is fully consumed. Hence, further increasing the temperature does not affect the carbon conversion [40]. The current result is in line with the results reported by Billaud et al. [39] for wood biomass gasification using steam and CO₂ reactants. Noticeably, at an ER of 0.99 (nearly combustion), the carbon conversion is 100% even at a temperature of 800 °C, due to the assumption of infinite residence time to reach equilibrium.

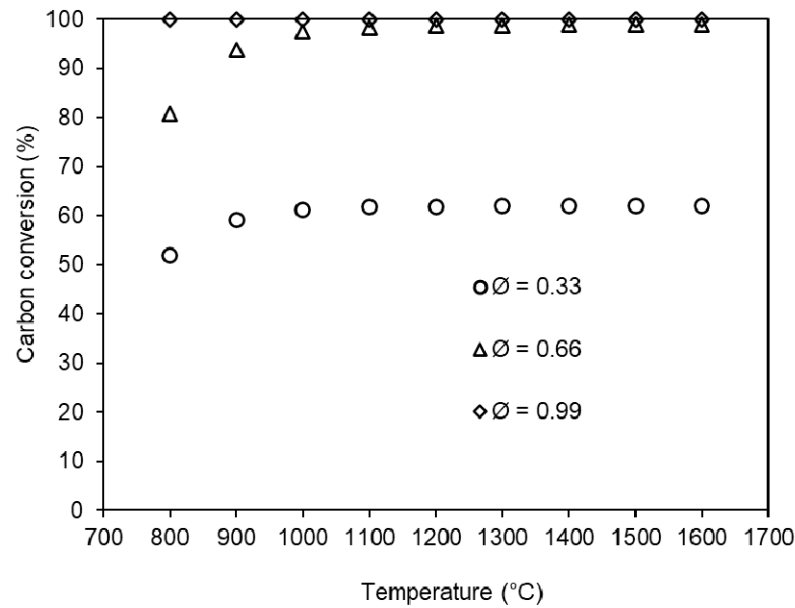


Figure 3. Effect of temperature on carbon conversion using different equivalence ratios at atmospheric pressure.

The effect of ER on syngas composition is shown in Figure 4. It is observed that increasing the ER increases the yield of CO up to the ER of 0.66 due to the favoured endothermic Boudouard (Equation (1)) and steam gasification (Equation (2)) reactions [41]. However, the yield of H₂ decreases consistently [42] with increasing ER, primarily due to the reverse water gas shift reaction (Equation (4)) [43,44].

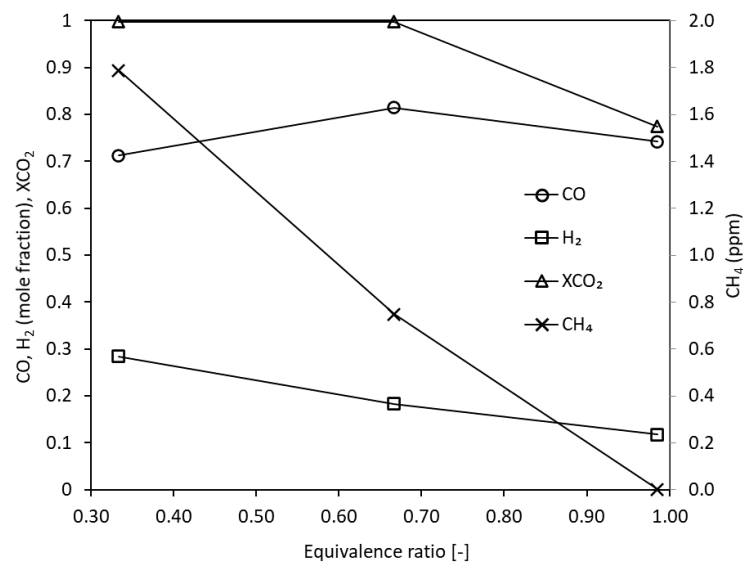


Figure 4. Effect of equivalence ratio on syngas composition.

The yield of CH₄ was negligible, which decreases with increasing ER due to the favoured steam methane reforming reaction (Equation (5)) [45]. The conversion of CO₂ (X_{CO₂}) was 100% at an ER of 0.66, which dropped to 74% at an ER of 0.99 due to the complete carbon conversion. Similar results have been reported in the literature using different reactants and fuel types [39,41,46]. The results reveal that an ER of 0.33 is most favourable in this study due to significantly higher H₂ concentration. It is to be noted that the higher the H₂ concentration in syngas, the better the quality is, due to an at least ten times higher heating value compared to CO on a mass basis [22]. Commercial entrained

flow gasifiers using steam and oxygen are operated with an ER of <0.5 , mostly between 0.3 and 0.4 [45,47]. Hence, the rest of the analysis in the study is conducted under the ER of 0.33.

3.2. Effect of Temperature on the Gasification Performance of Pure Coal

The effect of temperatures on gas composition and CO_2 conversion (X_{CO_2}) is shown in Figure 5. The modelling was conducted over 800–1600 °C at atmospheric pressure. The result shows that increasing temperature increases the concentration of CO and H_2 until CO_2 conversion becomes $\sim 100\%$ at around 1100 °C, similar to the findings reported in Ref. [18]. At 1100 °C, the yield of CO and H_2 reaches a steady state, indicating that the process reaches equilibrium. The total concentration of CO, H_2 and CH_4 were summed to 0.99%. The yield of CO was 60% higher than that of H_2 , leading to the ratio of H_2/CO at ~ 0.40 under steady state conditions. In addition, the result indicates that the Boudouard reaction is more dominant compared to the water–gas shift reaction.

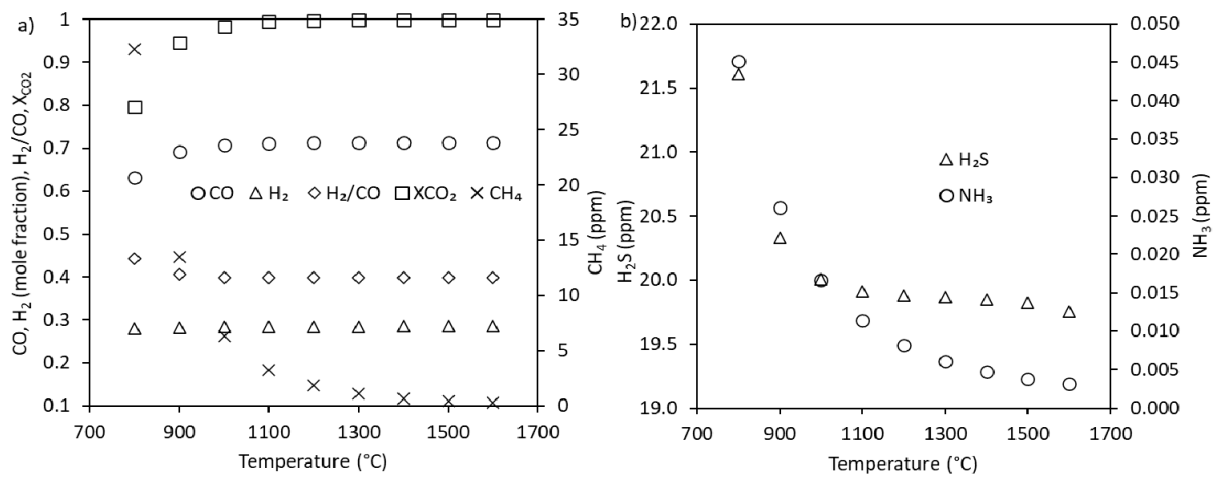


Figure 5. Effect of temperature on gas composition. (a) CO, H_2 , H_2/CO and X_{CO_2} ; (b) H_2S and NH_3 .

The yield of CH_4 is negligible, which decreases exponentially with increasing temperature [44]. The yield of pollutants such as H_2S and NH_3 are presented in Figure 5b. It is revealed that the yield of NH_3 decreases exponentially with increasing temperature, while the H_2S remains constant. The results indicate that a gasifier temperature of 1100 °C might be feasible for the gasification of current coal with an adjustment of residence time. A mass balance for PB0 gasification with respect to different temperatures and atmospheric pressure is shown in Table 5. The results show a good match between input and out mass flow rate with insignificant variation, which might be due to a calculation error.

Table 5. Mass balance for the gasification of pure coal (PB0) at different temperatures and atmospheric pressure.

T_g (°C)	PB0 (kg/h)	Feed CO_2 (kg/h)	Total in (kg/h)	CO (kg/h)	H_2 (kg/h)	CH_4 (kg/h)	CO_2 (kg/h)	H_2O (kg/h)	H_2S (kg/h)	NH_3 (kg/h)	Unconverted C (kg/h)	Ash (kg/h)	Total Out (kg/h)
800	100	110	210.0	134.62	4.25	0.39	20.35	3.35	0.56	0.0006	35.56	11.6	210.7
900	100	110	210.0	157.19	4.55	0.17	5.36	1.11	0.56	0.0004	30.14	11.6	210.7
1000	100	110	210.0	163.17	4.65	0.08	1.52	0.40	0.56	0.0002	28.69	11.6	210.7
1100	100	110	210.0	164.83	4.69	0.04	0.51	0.17	0.56	0.0002	28.29	11.6	210.7
1200	100	110	210.0	165.36	4.70	0.02	0.20	0.08	0.55	0.0001	28.16	11.6	210.7
1300	100	110	210.0	165.56	4.71	0.01	0.09	0.04	0.55	0.0001	28.11	11.6	210.7
1400	100	110	210.0	165.65	4.71	0.01	0.05	0.02	0.55	0.0001	28.09	11.6	210.7
1500	100	110	210.0	165.69	4.72	0.01	0.03	0.01	0.55	0.0001	28.08	11.6	210.7
1600	100	110	210.0	165.71	4.72	0.00	0.02	0.01	0.55	0.0000	28.08	11.6	210.7

3.3. Effect of Pressure on the Gasification Performance of Pure Coal

The effect of pressure on syngas and CO₂ conversion at different temperatures is shown in Figure 6. The result depicts that pressure plays a significant role at a lower temperature under non-steady state conditions. However, upon reaching a steady state, a minor effect is observed [41]. At a temperature of 800 °C, the concentration of CO at one bar was 0.63, which decreased exponentially at 0.26 with increasing pressure at 30 bar. The result can be explained as the conversion of CO₂, which decreases with increasing pressure [41]. On the other hand, at a temperature of 1200 °C, the yield of CO decreases slightly with increasing pressure as reactions reach equilibrium [48].

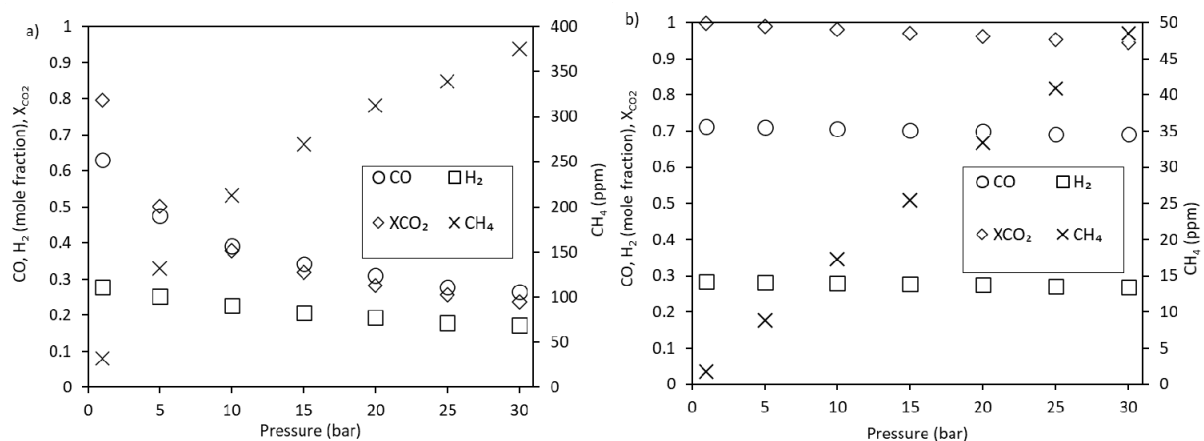


Figure 6. The effect of pressure on syngas composition and CO₂ conversion at two different temperatures of (a) 800 °C and (b) 1200 °C.

As the pressure increases, the hydrogenation of CO and CO₂ become dominant [49]. In addition, the consumption of H₂ increases due to the water–gas shift reaction. In contrast, the production of CH₄ increases with increasing pressure, and results from the favoured Sabatier reaction in reverse direction [22]. Overall, the effect of pressure on syngas composition is significant before reaching the process steady state, i.e., at a temperature below 1100 °C. The effect of the biomass blending ratio reported in the next section has been tested under atmospheric pressure, similar to the pilot-scale study reported in Ref. [47] for entrained flow gasification of lignites.

3.4. Effect of Blending Ratio on The Co-Gasification Performance

Figure 7 shows the effect of coal and biomass blending ratio on syngas composition. As observed in Figure 7a, increasing the biomass concentration in the blend decreases the yield of CO. However, a drastic decrease in CO was observed with a blending ratio above 50%.

Above 1100 °C, the addition of biomass with 20%, 50% and 80% leads to a decrease in the CO concentration by 0.7, 1.1 and 5.3 percentage points, respectively. Compared to pure coal, pure biomass resulted in a decrease in CO by 10 percentage points. The decrease in CO with increasing biomass ratio is presumably due to the decrease in carbon content in the sample [26]. A decrease in carbon content in the samples between 9.0% and 27% results in the decrease of CO by 1.0 to 10 percentage points. However, further research to fully elucidate the cause of this phenomenon is sought. The conversion of CO₂ follows a similar trend to that of CO, meaning that the variation in conversion is negligible below PB50, while significant over a biomass ratio of 50% (Figure 7h).

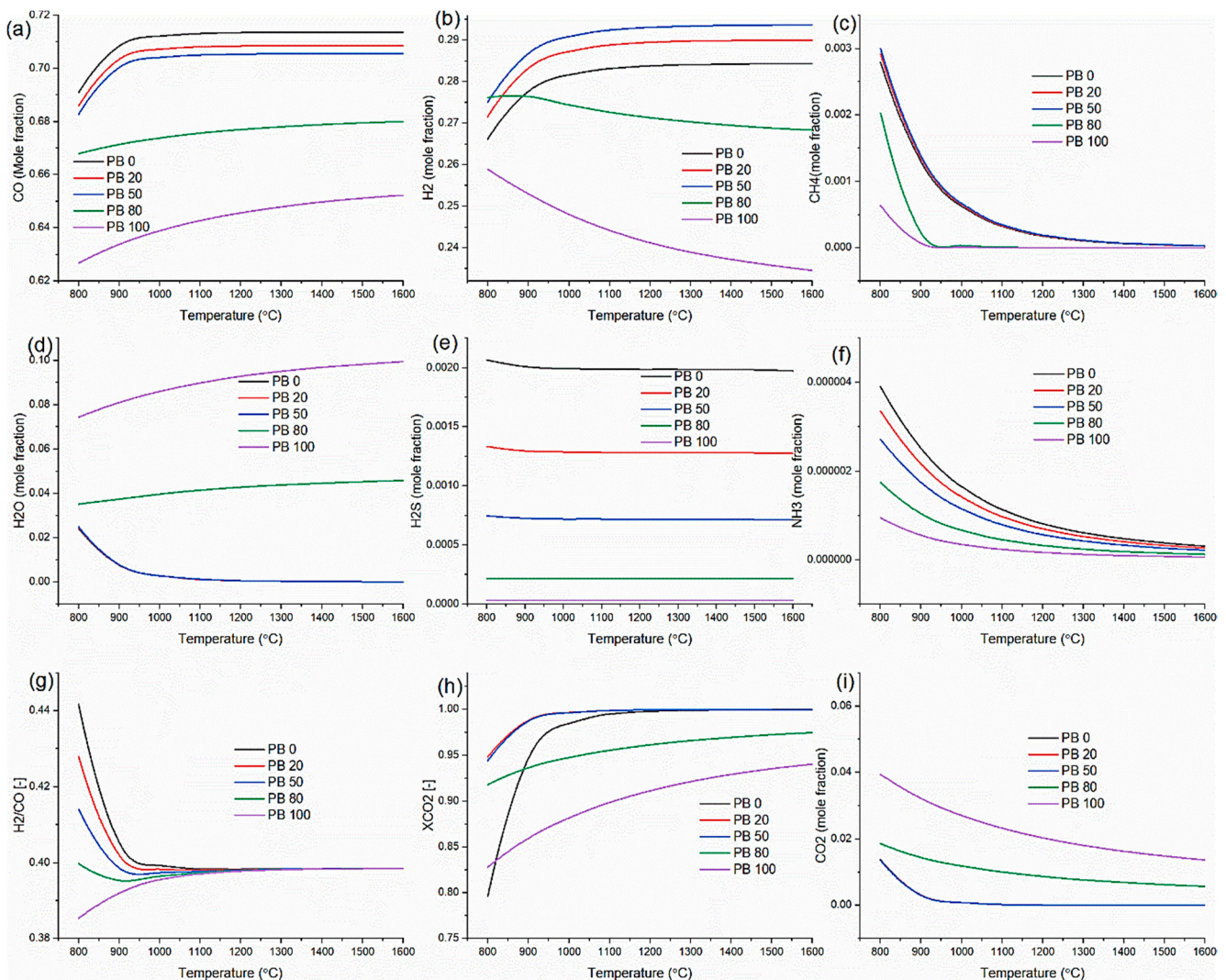


Figure 7. Effect of coal and biomass ratio on syngas composition and CO₂ conversion at different temperatures: PB0: black, PB20: red, PB50: blue, PB80: green, PB100: purple. (a) CO; (b) H₂; (c) CH₄; (d) H₂O; (e) H₂S; (f) NH₃; (g) H₂/CO; (h) X_{CO2}; (i) CO₂.

According to Figure 7b, increasing biomass ratio leads to an increase in the concentration of H₂, reaching a maximum at PB50. Further increasing the biomass leads to a decrease in the concentration of H₂ significantly, particularly for pure biomass. The increase in H₂ yield up to PB50 might be explained by the higher gasification rate and higher concentration of H in biomass [38]. Increasing H₂ concentration with increasing biomass ratio is reported in the literature [50]. However, a thorough study to find the cause of reduction in H₂ yield using biomass over PB50 needs to be undertaken in the future.

The syngas composition reaches a steady state at 1100 °C with an H₂/CO ratio of about 0.40 (Figure 7g). According to Figure 7c, the yield of CH₄ was negligible, with almost no difference up to PB50. However, using PB80 and PB10, the concentration of CH₄ decreases drastically and become almost nil at a temperature over 900 °C. The concentration of H₂O overlapped among PB0, PB20 and PB50, above which an increase with increasing the biomass ratio was observed (Figure 7d). The final compositions of CH₄ and H₂O are governed by the reverse water–gas shift and Sabatier reactions.

The yield of two pollutants—H₂S and NH₃—decrease with increasing biomass concentration, which is in the ppm range (Figure 7e,f). The pollutant emission from pure biomass is nearly zero. A proportional relationship between inherent N and S content and with those of NH₃ and H₂S is observed. While comparing coal and biomass, the N and S content

in biomass are 10 and 50 times lower than in coal. Thus, increasing biomass concentration in the blend results in the decrease of H_2S and NH_3 . The overall gas composition suggests that biomass blending up to 50% is optimum for the fuels studied.

Figure 8 shows the effect of biomass ratio on total syngas, LHV and CGE. It is observed that increasing biomass ratio increases the total syngas flow rate up to PB50. Further increasing the biomass in the blend leads to a decrease in the total syngas flow rate due to the significant decrease in carbon for gasification reactions [26]. The LHV overlaps each other among PB0, PB20 and PB50 due to the insignificant variation in the concentration of CO and H_2 . However, increasing the biomass ratio above 50% results in the decrease of LHV consistently [38]. A maximum LHV of 12 MJ/kg and a CGE of 78% was determined using PB50. Due to the insignificant difference in LHV among the samples, the CGE is predominantly governed by total syngas yield at different biomass ratios. Figure 8d shows the relationship among CGE, the total syngas and temperature using PB50. It is revealed that increasing temperature increases the total syngas flow rate and thereby the CGE [7].

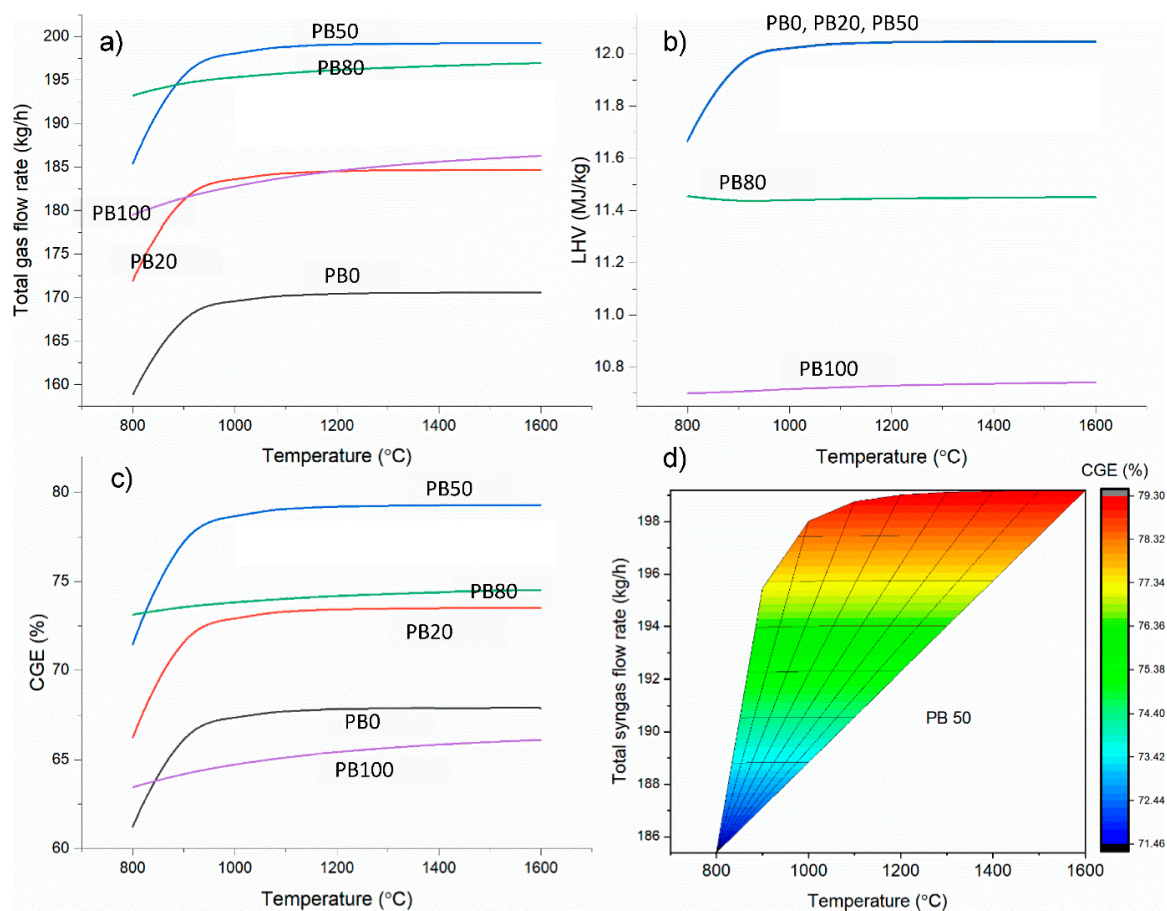


Figure 8. Effect of biomass ratio on total gas flow rate, LHV and CGE at different temperatures (a) total gas flow rate for all samples; (b) LHV; (c) CGE; (d) total gas flow rate and CGE for PB50.

4. Conclusions

In this study, an assessment of coal and biomass co-gasification has been carried out using Aspen plus process simulator. The effect of equivalence ratio, temperature, pressure and biomass to coal ratio have been investigated using CO_2 reactant. The results show that increasing temperature increases the yield of CO and H_2 up to the steady state temperature (1100 °C). The pressure effect is significant only at a lower temperature (<1100 °C), considering syngas composition. Increasing biomass ratio up to 50% in the blends increases the concentration of H_2 , above which a significant drop appears. However, the concentration of CO decreases consistently with increasing biomass ratio in the blend, with very

little variation up to 50% biomass. The blended sample with 50% biomass resulted in a maximum LHV of 12 MJ/kg and a CGE of 78%. The concentration of pollutants decreased consistently with increasing biomass ratio. Thus, co-gasification using CO₂ reactants can potentially increase gasification efficiency besides reducing pollutant emissions.

Author Contributions: Conceptualization, M.S.; Formal analysis, M.S.; Investigation, M.S.; Methodology, M.S.; Project administration, S.B.; Supervision, S.B.; Validation, M.S.; Writing—original draft, M.S.; Writing—review & editing, M.S. and S.B. All authors have read and agreed to the published version of the manuscript.

Funding: This research received no external funding.

Conflicts of Interest: The authors declare no conflict of interest.

References

1. Le Quéré, C.; Andrew, R.M.; Canadell, J.G.; Sitch, S.; Korsbakken, J.I.; Peters, G.P.; Manning, A.C.; Boden, T.A.; Tans, P.P.; Houghton, R.A.; et al. Global carbon budget 2016. *Earth Syst. Sci. Data* **2016**, *8*, 1–45. [\[CrossRef\]](#)
2. Bouckaert, S.; Pales, A.F.; McGlade, C.; Remme, U.; Wanner, B.; Varro, L.; D'Ambrosio, D.; Thomas, S. *Net Zero by 2050: A Roadmap for the Global Energy Sector*; International Energy Agency Report: Paris, France, 2021.
3. Ng, K.S.; Lopez, Y.; Campbell, G.M.; Sadhukhan, J. Heat integration and analysis of decarbonised IGCC sites. *Chem. Eng. Res. Des.* **2010**, *88*, 170–188. [\[CrossRef\]](#)
4. Ayub, H.; Park, S.; Binns, M. Biomass to Syngas: Modified Non-Stoichiometric Thermodynamic Models for the Downdraft Biomass Gasification. *Energies* **2020**, *13*, 5668. [\[CrossRef\]](#)
5. Ferreira, S.; Monteiro, E.; Brito, P.; Vilarinho, C. A Holistic Review on biomass gasification modified equilibrium models. *Energies* **2019**, *12*, 160. [\[CrossRef\]](#)
6. Ahmed, I.; Gupta, A. Characteristics of cardboard and paper gasification with CO₂. *Appl. Energy* **2009**, *86*, 2626–2634. [\[CrossRef\]](#)
7. Oh, G.; Ra, H.W.; Yoon, S.M.; Mun, T.Y.; Seo, M.W.; Lee, J.G.; Yoon, S.J. Gasification of coal water mixture in an entrained-flow gasifier: Effect of air and oxygen mixing ratio. *Appl. Therm. Eng.* **2018**, *129*, 657–664. [\[CrossRef\]](#)
8. Renganathan, T.; Yadav, M.; Pushpavanam, S.; Voolapalli, R.; Cho, Y. CO₂ utilisation for gasification of carbonaceous feedstocks: A thermodynamic analysis. *Chem. Eng. Sci.* **2012**, *83*, 159–170. [\[CrossRef\]](#)
9. Kirtania, K.; Bhattacharya, S. CO₂ gasification behavior of biomass chars in an entrained flow reactor. *Biomass Convers. Biorefin.* **2016**, *6*, 49–59. [\[CrossRef\]](#)
10. Xu, T.; Bhattacharya, S. Entrained flow gasification behaviour of Victorian brown coal char at low temperature. *Fuel* **2018**, *234*, 549–557. [\[CrossRef\]](#)
11. Sircar, I.; Sane, A.; Wang, W.; Gore, J.P. Experimental and modeling study of pinewood char gasification with CO₂. *Fuel* **2014**, *119*, 38–46. [\[CrossRef\]](#)
12. Nilsson, S.; Gómez-Barea, A.; Ollero, P. Gasification of char from dried sewage sludge in fluidised bed: Reaction rate in mixtures of CO₂ and H₂O. *Fuel* **2013**, *105*, 764–768. [\[CrossRef\]](#)
13. Tanner, J.; Bhattacharya, S. Kinetics of CO₂ and steam gasification of Victorian brown coal chars. *Chem. Eng. J.* **2016**, *285*, 331–340. [\[CrossRef\]](#)
14. Chmielniak, T.; Sciazko, M.; Tomaszewicz, G.; Tomaszewicz, M. Pressurized CO₂-enhanced gasification of coal. *J. Therm. Anal. Calorim.* **2014**, *117*, 1479–1488. [\[CrossRef\]](#)
15. Shahabuddin, M.; Bhattacharya, S. Effect of reactant types (steam, CO₂ and steam+ CO₂) on the gasification performance of coal using entrained flow gasifier. *Int. J. Energy Res.* **2021**, *45*, 9492–9501. [\[CrossRef\]](#)
16. Shahabuddin, M.; Kibria, M.A.; Bhattacharya, S. Effect of pore diffusion on the gasification characteristics of coal char under CO₂ atmosphere. *Int. J. Energy Clean Environ.* **2021**, *22*, 85–102. [\[CrossRef\]](#)
17. Irfan, M.F.; Usman, M.R.; Kusakabe, K. Coal gasification in CO₂ atmosphere and its kinetics since 1948: A brief review. *Energy* **2011**, *36*, 12–40. [\[CrossRef\]](#)
18. Sadhwani, N.; Li, P.; Eden, M.R.; Adhikari, S. *Process Modeling of Fluidized Bed Biomass-CO₂ Gasification using ASPEN Plus*. *Computer Aided Chemical Engineering*; Elsevier: Amsterdam, The Netherlands, 2017; pp. 2509–2514.
19. Li, H.; Yu, Y.; Han, M.; Lei, Z. Simulation of coal char gasification using O₂/CO₂. *Int. J. Coal Sci. Technol.* **2014**, *1*, 81–87. [\[CrossRef\]](#)
20. Klimanek, A.; Bigda, J. CFD modelling of CO₂ enhanced gasification of coal in a pressurised circulating fluidised bed reactor. *Energy* **2018**, *160*, 710–719. [\[CrossRef\]](#)
21. Shahabuddin, M.; Krishna, B.B.; Bhaskar, T.; Perkins, G. Advances in the thermo-chemical production of hydrogen from biomass and residual wastes: Summary of recent techno-economic analyses. *Bioresour. Technol.* **2020**, *299*, 122557. [\[CrossRef\]](#)
22. Shahabuddin, M.; Bhattacharya, S. Process modelling for the production of hydrogen-rich gas from gasification of coal using oxygen, CO₂ and steam reactants. *Int. J. Hydrogen Energy* **2021**, *46*, 24051–24059. [\[CrossRef\]](#)
23. Ng, K.S.; Zhang, N.; Sadhukhan, J. Techno-economic analysis of polygeneration systems with carbon capture and storage and CO₂ reuse. *Chem. Eng. J.* **2013**, *219*, 96–108. [\[CrossRef\]](#)

24. Shahabuddin, M.; Bhattacharya, S.; Srivatsa, S.C. Co-slagging characteristics of coal and biomass ashes considering entrained flow slagging gasifier. *Biomass Convers. Biorefin.* **2021**, 1–10. [CrossRef]
25. Ali, D.A.; Gadalla, M.; Abdelaziz, O.; Hultheberg, C.P.; Ashour, F.H. Co-gasification of coal and biomass wastes in an entrained flow gasifier: Modelling, simulation and integration opportunities. *J. Nat. Gas Sci. Eng.* **2017**, *37*, 126–137. [CrossRef]
26. Kuo, P.-C.; Wu, W. Thermodynamic analysis of a combined heat and power system with CO₂ utilisation based on co-gasification of biomass and coal. *Chem. Eng. Sci.* **2016**, *142*, 201–214. [CrossRef]
27. Castaldi, M.; Dooher, J. Investigation into a catalytically controlled reaction gasifier (CCRG) for coal to hydrogen. *Int. J. Hydrogen Energy* **2007**, *32*, 4170–4179. [CrossRef]
28. Aspen Plus. *Aspen Plus User Guide, Version 10.2*; Aspen Technology: Burlington, MA, USA, 2010; Chapter 10; pp. 2–28.
29. Marcantonio, V.; Bocci, E.; Monarca, D. Development of a chemical quasi-equilibrium model of biomass waste gasification in a fluidised-bed reactor by using Aspen Plus. *Energies* **2020**, *13*, 53. [CrossRef]
30. Yoshida, H.; Kiyono, F.; Tajima, H.; Yamasaki, A.; Ogasawara, K.; Masuyama, T. Two-stage equilibrium model for a coal gasifier to predict the accurate carbon conversion in hydrogen production. *Fuel* **2008**, *87*, 2186–2193. [CrossRef]
31. Xiangdong, K.; Zhong, W.; Wenli, D.; Feng, Q. Three stage equilibrium model for coal gasification in entrained flow gasifiers based on aspen plus. *Chin. J. Chem. Eng.* **2013**, *21*, 79–84.
32. Visconti, A.; Miccio, M.; Juchelková, D. An aspen plus tool for simulation of lignocellulosic biomass pyrolysis via equilibrium and ranking of the main process variables. *Int. J. Math. Models Methods Appl. Sci.* **2015**, *9*, 71–86.
33. Suwaththikul, A.; Limprachaya, S.; Kittisupakorn, P.; Mujtaba, I.M. Simulation of steam gasification in a fluidised bed reactor with energy self-sufficient condition. *Energies* **2017**, *10*, 314. [CrossRef]
34. Dai, Z.; Gong, X.; Guo, X.; Liu, H.; Wang, F.; Yu, Z. Pilot-trial and modeling of a new type of pressurised entrained-flow pulverised coal gasification technology. *Fuel* **2008**, *87*, 2304–2313. [CrossRef]
35. Zhang, Z.F.; Tang, L.Y.; Lu, Q.Y.; Zhang, W.X.; He, Z.Z.; BI, D.H. Pulverised coal gasification simulation based on aspen plus software. *Chem. Fertil. Des.* **2008**, *3*. Available online: http://en.cnki.com.cn/Article_en/CJFDTOTAL-HFSJ200803004.htm (accessed on 4 November 2021).
36. Barrera-Zapata, R.; Salazar, C.; Pérez, J.F. Thermochemical Equilibrium Model of Synthetic Natural Gas Production from Coal Gasification Using Aspen Plus. *Int. J. Chem. Eng.* **2014**, *2014*, 1–18. [CrossRef]
37. Shahabuddin, M.; Kibria, M.; Bhattacharya, S. Evaluation of high-temperature pyrolysis and CO₂ gasification performance of bituminous coal in an entrained flow gasifier. *J. Energy Inst.* **2020**, *94*, 294–309. [CrossRef]
38. Shahabuddin, M.; Bhattacharya, S. Enhancement of performance and emission characteristics by co-gasification of biomass and coal using an entrained flow gasifier. *J. Energy Inst.* **2021**, *95*, 166–178. [CrossRef]
39. Billaud, J.; Valin, S.; Peyrot, M.; Salvador, S. Influence of H₂O, CO₂ and O₂ addition on biomass gasification in entrained flow reactor conditions: Experiments and modelling. *Fuel* **2016**, *166*, 166–178. [CrossRef]
40. Tanner, J. High Temperature, Entrained Flow Gasification of Victorian Brown Coals and Rhenish Lignites. Ph.D. Thesis, Monash University, Clayton, Australia, 2015.
41. Adnan, M.A.; Hossain, M.M. Gasification performance of various microalgae biomass—A thermodynamic study by considering tar formation using Aspen plus. *Energy Convers. Manag.* **2018**, *165*, 783–793. [CrossRef]
42. Villarini, M.; Marcantonio, V.; Colantoni, A.; Bocci, E. Sensitivity Analysis of Different Parameters on the Performance of a CHP Internal Combustion Engine System Fed by a Biomass Waste Gasifier. *Energies* **2019**, *12*, 688. [CrossRef]
43. Adnan, M.A.; Hossain, M.M. Gasification of various biomasses including microalgae using CO₂—A thermodynamic study. *Renew. Energy* **2018**, *119*, 598–607. [CrossRef]
44. Pala, L.P.R.; Wang, Q.; Kolb, G.; Hessel, V. Steam gasification of biomass with subsequent syngas adjustment using shift reaction for syngas production: An Aspen Plus model. *Renew. Energy* **2017**, *101*, 484–492. [CrossRef]
45. Doherty, W.; Reynolds, A.; Kennedy, D. The effect of air preheating in a biomass CFB gasifier using ASPEN Plus simulation. *Biomass Bioenergy* **2009**, *33*, 1158–1167. [CrossRef]
46. Turn, S.; Kinoshita, C.; Zhang, Z.; Ishimura, D.; Zhou, J. An experimental investigation of hydrogen production from biomass gasification. *Int. J. Hydrogen Energy* **1998**, *23*, 641–648. [CrossRef]
47. Ünlü, A.; Kayahan, U.; Argönül, A.; Ziypak, M.; Akça, A. Pilot scale entrained flow gasification of Turkish lignites. *J. Energy Inst.* **2017**, *90*, 159–165. [CrossRef]
48. Molino, A.; LaRocca, V.; Chianese, S.; Musmarra, D. Biofuels Production by Biomass Gasification: A Review. *Energies* **2018**, *11*, 811. [CrossRef]
49. AlNouss, A.; McKay, G.; Al-Ansari, T. Production of syngas via gasification using optimum blends of biomass. *J. Clean. Prod.* **2020**, *242*, 118499. [CrossRef]
50. Li, K.; Zhang, R.; Bi, J. Experimental study on syngas production by co-gasification of coal and biomass in a fluidised bed. *Int. J. Hydrogen Energy* **2010**, *35*, 2722–2726. [CrossRef]